www.icgst.com

Design and Analysis of a Robust Accurate Speed Control System by Applying a Digital Compensator

Kamen M. Yanev[1]
Department of Electrical Engineering, University of Botswana, Gaborone, Botswana
yanevkm@yahoo.com, yanevkm@mopipi.ub.bw
http://www.ub.bw/

Abstract

This paper provides further advancement of the D-Partitioning analysis applied to nonlinear digital control system with variable parameters. As a case study, a nonlinear control system for accurate speed control of a dc motor is considered. The Bilinear Tustin Transform method is employed as one of the most precise facilities for systems discretization, where also the Euler's approximation is taken into account. A robust controller design is accomplished by a number of successive steps. Based on the difference equations of its stages, the robust controller can be realized by microcontrollers. The research is a further development of the author's work on the D-Partitioning analysis and design of nonlinear digital control systems with variable parameters. The suggested tool for analysis is essential and beneficial for the further development of control theory in this area.

Keywords: *Wheatstone Speed-to-Voltage Converter, Speed Control, Nonlinear, Bilinear approximation, Discretization, D-Partitioning Stability Analysis, Digital Control Systems;*

Nomenclature

WSVC	Wheatstone Speed-to-Voltage Converter
BC	Bridge Converter
WB	Wheatstone bridge
M	DC Motor
V_{fb}	Feedback signal
E	emf of the dc motor's armature
T_L	Variable load torque applied to the dc motor
n	Speed of the dc motor
RCU	Reference and Comparison Unit
V_r	Reference voltage
Φ	Output nonlinear signal of the comparator
VPPG	Variable-phase pulse generator
CG	Current Generator
TU	Threshold Unit
α	Controlled thyristor-firing angles
$G_P(s)$	Transfer function of open-loop linear section
s	Laplace operator
K	Variable gain of the linear section of the system
$N(M)$	Describing function of the system's nonlinearity
T_s	Sampling period
T_{min}	Minimum time-constant of the linear section of the system
ω_S	Sampling frequency
z	z-transform operator
K_1	Saturation factor of the nonlinear element
h	Hysteresis factor of the nonlinear element
m, n	Input and output of the nonlinear element
$G_{CL0}(s)$	Transfer function of closed-loop linear section Type 0
ζ	Closed-loop relative damping ratio
$G_S(s)$	Transfer function of the series robust controller
$G_F(s)$	Transfer function of the forward controller
$G_T(s)$	Transfer function of the robust control system
$G_{dS}(z)$	Transfer function of the series robust controller stage in the discrete-time domain
$G_{dF}(z)$	Transfer function of the forward robust controller stage in the discrete-time domain
$U(z)$	Output of the digital series controller stage
$X(z)$	Input of the digital series controller stage
$E(z)$	Output of the digital forward controller stage
$V(z)$	Input of the digital forward controller stage
IP	Performance index used in adaptive control

1. Introduction

The current research presents a strategy for analysis and design of a digital robust control system for accurate speed control of a dc motor. Control system, maintaining constant motor speed, should contain a speed-to-voltage converter in its feedback loop. As an innovative solution of the problem, it is suggested the incorporation of a Wheatstone bridge that is to operate as a speed-to-voltage converter. In the Wheatstone Speed-to-Voltage Converter (WSVC) the armature circuit of a separately excited dc motor is connected as one of the arms of a Wheatstone bridge. The advantage of the WSVC is that its output voltage depends directly on the armature emf and therefore on the speed of the dc motor.

To maintain constant motor speed, the WSVC is involved in a feedback control system. It consists of a linear part

and a non-linear part that is an on-off element with hysteresis. The system can also become independent of parameter variations, if a digital robust controller, based on microcontrollers is implemented [1]. The strategy for analysis of digital control system is achieved with the aid of the D-Partitioning [2], [3] and by introducing discretization based on the Bilinear Tustin Transform [4]. The system's sampling time is selected, based on consideration of the Euler's approximation [5], [6].

This research is a further progress of the author's work in the area of the Advanced D-Partitioning analysis of digital control systems with variable parameters. It demonstrates that the Advanced D-Partitioning analysis, for linear continuous-time systems [7], can be also applied for nonlinear digital control systems.

For the clarity of the presented research, this paper is organized in the following sequence. Initially, the structure of a speed control system utilizing a WSVC is described, followed by the stability analysis of the system's linear section. The method of the Advanced D-Partitioning analysis is described and implemented in the discrete-time domain in terms of the variable system's gain. Next, after the nonlinear section of the system is represented, the Goldfarb Stability Criterion, known also as the Describing Function Analysis is applied [7], [8]. It is based on the interaction of the linear and the nonlinear section of the system and it determines the stability of the total control system, as well as its robustness. Further, the design steps and the application of a robust controller are revealed. Finally the achieved system robustness and precise speed control of the dc motor are demonstrated.

2. Structure of the Speed Control System Employing a WSVC

To achieve accurate-speed control of a dc motor, the armature of the separately excited dc motor is connected as one of the ratio arms of a Wheatstone bridge. The interaction of the dc motor and the Wheatstone bridge, as shown in Figure 1, is a unique arrangement, proposed by the author that can be specified as a Wheatstone Speed-to-Voltage Converter (WSVC). The bridge is originally balanced at static armature conditions when only the motor armature resistance participates in the bridge ratio arm. Under running conditions of the motor, the bridge becomes unbalanced and its output voltage, depending directly to the motor speed, is continuously compared with a preset reference voltage.

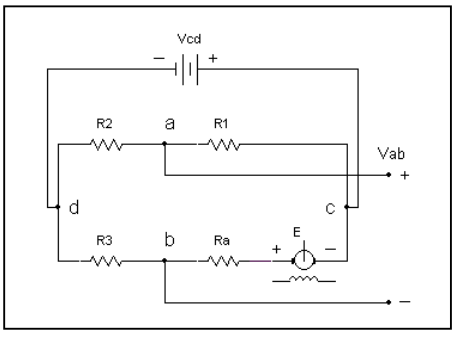

Figure 1. Wheatstone Speed-to-Voltage Converter (WSVC)

The block diagram of the closed loop control system is shown in Figure 2. The supply ac line voltage V is applied to a thyristor Bridge Converter (BC). The variable rectified voltage of the BC V_{cd} is applied to a Wheatstone bridge (WB). The armature of the dc motor (M) is connected as one of the arms of the (WB). The incorporation of the motor (M) and the (WB) is, as described, the unique new technical solution, considered as a Wheatstone Speed-to-Voltage Converter (WSVC).

The output voltage of the WSVC V_{fb} is a feedback signal that depends not only on the input bridge voltage V_{cd} but also on the motor's armature emf $E = V_{bc}$. Variable load torque T_L, applied to the motor, does not affect its speed n because of the tight closed-loop control.

The feedback voltage V_{fb} is applied to a Reference and Comparison Unit (RCU). There, it is compared with a reference voltage V_r which is developed within the RCU. The output signal Φ of the comparator controls the variable-phase pulse generator (VPPG). It consists of a Current Generator (CG) and a Threshold Unit (TU). The output voltage of the CG V_c is applied to TU in this way controlling the thyristor-firing angles α of the BC.

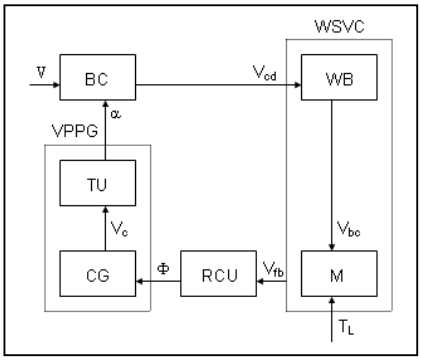

Figure 2. Block Diagram of the Accurate Speed Control System

3. Stability Analysis of the Linear Section and System Discretization

The linear section of the system consists of the elements: CG, TU, BC and WSVC. Considering the parameters of all system elements, the transfer function of the total open loop linear section, as a stand alone system is presented as:

$$G_P(s) = \frac{21.6K}{(1+0.01s)(1+0.03s)(1+0.042s)} = \\ = \frac{21600K}{0.0126s^3 + 1.98s^2 + 72s + 1000} \quad (1)$$

where K is the plant's gain, being a variable parameter

The nonlinearity in RCU is designed as an ON-OFF element with hysteresis, having a describing function $N(M)$. The total control system is a combination of a linear and a nonlinear part. The block diagram shown in Figure 3, introduces also a digital robust control that is incorporated into the control system.

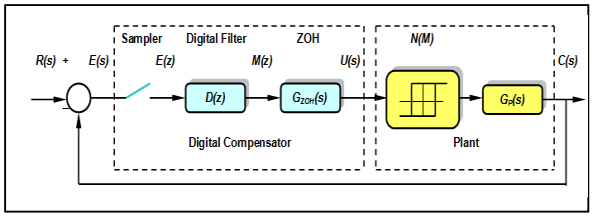

Figure 3. Block Diagram of the Digital Robust Control System

Considering application of digital robust control, in accordance to the Euler's approximation [5], [6], [9], the sampling period T_s of the discrete system, should be within the range $T_s \leq (0.1T_{min}$ to $0.2T_{min})$, where T_{min} is the minimum time-constant of the continuous-time system or the analogue plant model prototype. Only then there will be a close match between the discrete and the continuous-time system performance. In this case, the plant's minimum time constant is T_{min} = 0.01sec. Then the sampling period is chosen as T_s = 0.001 sec which satisfies the condition $T_s \leq 0.1T_{min}$.

Further, the method of the Advanced D-Partitioning is applied to analyze the stability of the linear section of the system. The initial ideas of an analysis categorized as method of D-Partitioning were suggested by Neimark [2], [10], [11] and is considered as a method of evaluation of linear system stability, when the system's parameters are variable. At its initial steps the method was stating rather its theoretical possibilities and its applications were quite limited.

In a number of previously published research [9], [12], [13], [14], [15], the author of this paper, further expanded the initial ideas of Neimark to a method of **Advanced D-Partitioning,** developing a generalized stability analysis tool. By implementing an interactive MATLAB procedure methodology, the Advanced D-Partitioning created by the author, is based on innovative transparent graphical display of regions of stability and instability in the space of system's variable parameters. The basic principle, suggested by the author, is introducing the system's characteristic equation in a format that exposes the variable parameter.

If the variable parameter is presented as a complex number, the D-Partitioning regions can be obtained graphically in the complex plane of this parameter, by varying the frequency within the range $-\infty \leq \omega \leq +\infty$. The D-Partitioning curve in terms of one variable parameter can be plotted in the complex plane within the frequency range $-\infty \leq \omega \leq +\infty$, facilitated by MATLAB the "nyquist" m-code.

To avoid any misinterpretation of the D-Partitioning procedure, the "nyquist" m-code is modified into a "dpartition" m-code with the aid of the MATLAB Editor and a proper formatting. The "dpartition" m-code can plot the curve of a specific system parameter in terms of the frequency variation from $-\infty$ to $+\infty$. In order to benefit from the Advanced D-Partitioning analysis suggested by the author, the wider engineering community can still use the "nyquist" m-code for the purpose of plotting the D-Partitioning curve.

The Advanced D-Partitioning analysis determines a number of regions in the variable parameter plane. When this analysis is **applied in the discrete-time domain, only the region that is always on the left-hand side of the D-Partitioning curve, for frequency variation within the range $\omega = \pm \omega_s/2 = \pm 2\pi/2T_s$, is the region of stability.** This is demonstrated, as shown below, by applying the Advanced D-Partitioning analysis to the case of the discussed system.

The Advanced D-Partitioning analysis is applied in the discrete-time domain with the aid of the **Bilinear Tustin Transform** [16], [17] that is a first-order approximation of the natural logarithm function, being an **exact mapping of the z-plane to the s-plane and vice versa**. It maps positions from the $j\omega$ axis in the s-plane to the unit circle |z| = 1 in the z-plane. The Bilinear Tustin approximation and its inverse are presented as:

$$z = e^{sT_s} = \frac{e^{sT_s/2}}{e^{-sT_s/2}} \approx \frac{1+sT_s/2}{1-sT_s/2};\ s = \frac{1}{T_s}\ln(z) \approx \frac{2}{T_s}\frac{z-1}{z+1} \qquad (2)$$

To employ the Bilinear Tustin Transform, the MATLAB *'tustin'* code is to be applied, performing the transform of the continuous-time to discrete-time system equivalents. In this case, taking into account the linear section of the plant, its gain K is considered as variable parameter. Following the steps of the Advanced D-Partitioning analysis, the characteristic equation of the continuous section of the plant is obtained from equation (1) as:

$$G(s) = 0.0126s^3 + 1.98s^2 + 72s + 1000 + 21600K = 0 \qquad (3)$$

The variable parameter K of the system's linear section is determined from equation (3) as follows:

$$K(s) = -\frac{0.0126s^3 + 1.98s^2 + 72s + 1000}{21600} \qquad (4)$$

Initially, the variable *K(s)* is introduced as a continuous function and next converted into its digital equivalent *K(z)* with the aid of the Bilinear Tustin Transform.

Further, the D-Partitioning is achieved in the discrete-time domain in terms of the variable gain K as follows:

```
>> K=tf([-0.0126 -1.98 -72 -1000],[0 21600])
Transfer function:
-0.0126 s^3 - 1.98 s^2 - 72 s - 1000
-----------------------------------
          21600
>> Kd1 = c2d(K,0.001,'tustin')
Transfer function:
-5040 z^3 + 1.436e004 z^2 - 1.363e004 z + 4307
---------------------------------------------
        z^3 + 3 z^2 + 3 z + 1
Sampling time: 0.001
>> dpartition(Kd1)
```

where

$$K(z) = \frac{-5040z^3 + 14360z^2 - 13630z + 4307}{z^3 + 3z^2 + 3z + 1} \qquad (5)$$

The D-Partitioning curve, plotted in the K-plane in the discrete-time domain, is considered within the frequency range $\omega = \pm \omega_s/2 = \pm 2\pi/2T_s = \pm 3141.6$ rad/sec.

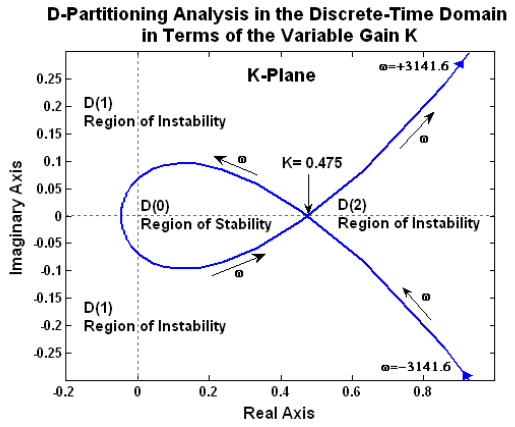

Figure 4: D-Partitioning Analysis in the Discrete-Time Domain of the Linear Section in Terms of the Variable Gain K

The D-Partitioning, as seen in Figure 4, determines three regions on the *K*-plane: D(0), D(1) and D(2). **Only D(0) is the region of stability, being always on the left-hand side of the curve.** The system will be stable only when its gain is within the range $0 \le K \le 0.475$. The negative part of the stability region D(0) is ignored, since the gain *K* may obtain only positive values. The performance of the entire system depends on the stability of the continuous linear section as a stand alone system. The overall system may become unstable if $K \ge 0.475$.

4. Describing Function Analysis in Case of ON-Off Element with Hysteresis

4.1. Characteristics of the Nonlinearity

The nonlinear section of the plant is an ON-OFF nonlinearity with hysteresis. Its transfer characteristic and its properties are shown in Figure 5.

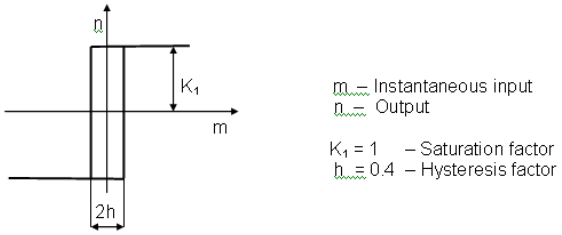

Figure 5: Characteristic of the ON-OFF Nonlinearity with Hysteresis

The describing function of the ON-OFF nonlinearity with hysteresis is presented as follows [18], [19]:

$$N(M) = \frac{4K_1}{\pi M} \angle -\sin^{-1}\left(\frac{h}{M}\right) \qquad (6)$$

where M is the amplitude of the input variations

In this case, the parameters of the nonlinearity ($K_1 = 1$ and $h = 0.4$) are considered as constant. The function $Z(M) = -1/N(M)$ is obtained by applying equation (6). The results for different amplitudes *M* are shown in Table 1.

Table 1

N(M) and *Z(M)* = *–1/N(M)* at Different Input Amplitudes *M*

(Case of ON-OFF Nonlinearity with Hysteresis; $K_1 = 1$ and $h = 0.4$)

M	0.4	0.8	1.6	2.4
N(M)	3.18∠–90°	1.59∠–30°	0.8∠–30°	0.53∠–10°
Z(M)	–0.31∠+90°	–0.63∠+30°	–1.25∠+14°	–1.9∠+10°

4.2. Applying the Describing Function Analysis

The results from the Advanced D-Partitioning analysis demonstrate that if $K \le 0.475$ the linear prototype section of the system $G_P(s)$ is stable. This is a required precondition for further applying the Describing Function Analysis, known also as the Goldfarb Stability Criterion. For this analysis, both $G_P(j\omega)$ equivalent prototype in the discrete-time domain, at different gains (K = 0.1, 0.25 and 0.4) and the nonlinear function $Z(M) = -1/N(M)$ are plotted simultaneously in the complex plane as seen in Figure 6. The following MATLAB code is applied:

```
>> Gp01=tf([0 2160],[0.0126 1.98 72 1000])
        Transfer function:
          2160
  ------------------------------
  0.0126 s^3 + 1.98 s^2 + 72 s + 1000
>> Gp025=tf([0 5400],[0.0126 1.98 72 1000])
Transfer function:
                5400
  ------------------------------
  0.0126 s^3 + 1.98 s^2 + 72 s + 1000
>> Gp04=tf([0 8640],[0.0126 1.98 72 1000])
Transfer function:
            8640
  ------------------------------
  0.0126 s^3 + 1.98 s^2 + 72 s + 1000
>> Gp1d=c2d(Gp01,0.001,'tustin')
Transfer function:
1.984e-005 z^3 + 5.952e-005 z^2 + 5.952e-005 z +  1.984e-005
  ------------------------------------------------------
          z^3 - 2.849 z^2 + 2.704 z - 0.8545
Sampling time: 0.001
>> Gp2d=c2d(Gp025,0.001,'tustin')
Transfer function:
4.96e-005 z^3 + 0.0001488 z^2 + 0.0001488 z + 4.96e-005
  ------------------------------------------------------
  z^3 - 2.849 z^2 + 2.704 z - 0.8545
Sampling time: 0.001
>> Gp3d=c2d(Gp04,0.001,'tustin')
Transfer function:
7.936e-005 z^3 + 0.0002381 z^2 + 0.0002381 z + 7.936e-005
  ------------------------------------------------------
    z^3 - 2.849 z^2 + 2.704 z - 0.8545
Sampling time: 0.001
>> nyquist(Gp1d,Gp2d,Gp3d)
```

If the $Z(M) = -1/N(M,\omega)$ locus and the $G_P(j\omega)$ locus intersect, the system output exhibits a sustained oscillation, or a limit cycle. Such a sustained oscillation is not sinusoidal, but it can be approximated by a sinusoidal one and is characterized by the magnitude *M* of the $Z(M) = -1/N(M,\omega)$ locus and the value of the frequency ω of the $G_P(j\omega)$ locus at the intersection point.

This is the natural and desirable operation of the system in case of nonlinearity of the type ON-OFF element with hysteresis. A limit cycle may be stable or unstable.

According to the Goldfarb stability criterion, the total control system is stable for each one of the discussed cases of different gains (K = 0.1, 0.25 and 0.4), since as seen from the Figure 6, each locus G_{P1d}, G_{P2d} or G_{P3d} is not enclosing the point (–1, j0) of the complex plane and also is not enclosing this part of the characteristic $Z(M)$, corresponding to the increment of M after a crossing point (M, ω), related to a limit cycle [7], [18], [19].

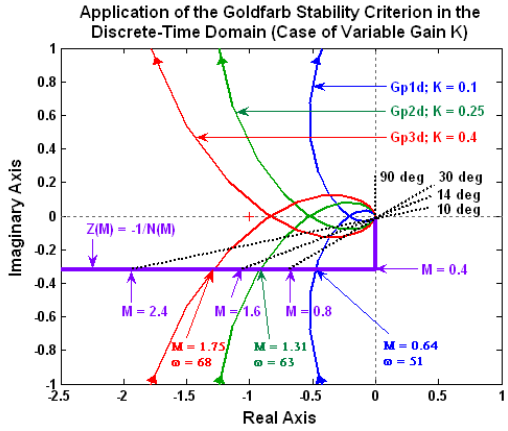

Figure 6: Goldfarb Stability Criterion in the Discrete-Time Domain at Linear Section Prototype Gains: K = 0.1, 0.25, and 0.4 (ON-OFF Nonlinearity with Hysteresis)

Due to the sensitivity to the variation of the linear section gain K, the stable limit cycles are with different amplitude M and frequency of oscillation ω as shown in Table 2.

Table 2
Frequency and Amplitude of Oscillations of the Stable limit Cycles at Different Values of the Gain K

Linear System Gain	*K*	0.1	0.25	0.4
Limit Cycles Properties	*M*	0.64	1.31	1.75
	ω, rad/sec	51	63	68

5. Design of a Digital Robust Controller

5.1. Choice between Adaptive or Robust Control

Adaptive control is a method that uses a controller which must adapt to a controlled system with variable or uncertain parameters [20]. When the parameters of a plant change considerably in time, following specific rule, the adaptive control approach is considered as the best option to achieve and maintain an acceptable level of control system performance [21].

An adaptive control system can be interpreted as a feedback system where the controlled variable is the performance index (IP). The measured IP will be compared to the desired IP and their difference will be fed into an adaptation mechanism. From their comparison, the adaptation mechanism modifies the parameters of the adjustable controller to generate a control signal in order to maintain the IP of the system close to the reference one [22]. The performance of the control system is adjusted by continuously modifying the parameters of the adaptive controller.

Although adaptive control improves the system's robust performance, **it cannot succeed in the presence of unstructured and unpredictable uncertainties.** Also it is recognized that it is complex and expensive. For this reason the adaptive control will not be considered in this research.

As alternative, an optimal robust controller can operate successfully if the system parameters increase or decrease in the range of 10 times with respect to their original values. The robust control does not need a priori information about the bounds on these uncertain parameters. Robust control guarantees that if the changes are within given bounds the control law need not be changed.

Also, a robust controller can be **applicable for unlimited number** of **unpredictable and random parameter variations disturbances and noise**. The application of robust control is considered quite sufficient in case of limited uncertainties. It is not as complex and it is less expensive compared with the adaptive control.

5.2. Design of the Robust Controller Stages

The current research is upgrading previous published work of the author [14], [15], [23], by suggesting a number of unique successive steps for design of optimal digital robust controller by applying forward-series compensation with two degrees of freedom.

The procedure is applied to the linear section prototype of the plant. The objective of the robust controller design is the robust control system to become a system with two enforced dominant poles that satisfy specific performance criteria. To achieve this objective, the following design steps are considered:

Stage 1: The closed-loop transfer function of the linear section of the plant as a stand alone system is determined from equation (1) as follows:

$$G_{CL_O}(s) = \frac{21600K}{0.0126s^3 + 1.89s^2 + 72s + 1000 + 21600K} \qquad (7)$$

Stage 2: The optimal value of the gain K, corresponding to the closed-loop relative damping ratio ζ = 0.707 that satisfies the selected ITAE performance index [24], is determined by the following code and interactive MATLAB procedure:

```
>> K=[0:0.0001:0.11];
>> for n=1:length(K)
G_array(:,:,n)=tf([21600*K(n)],[0.0126 1.89 72 1000+21600*K(n)]);
                    end
>> [y,z]=damp(G_array);
>> plot(K,z(1,:))
```

As seen from Figure 7, if the relative damping ratio is ζ = 0.7066 ≈ 0.707 the corresponding gain of the linear section of the system is K = 0.0153.

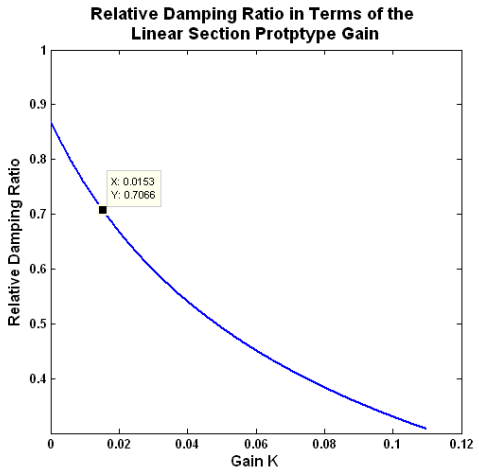

Figure 7: Determination of the Optimal Gain K

Stage 3: By substituting K = 0.0153 in equation (7) the transfer function of the closed-loop system is modified to:

$$G_{CL_O}(s) = \frac{330.48}{0.0126s^3 + 1.89s^2 + 72s + 1000 + 330.48} \quad (8)$$

This condition corresponds to the relative damping of ζ = 0.707 and to the desired closed-loop poles –22.4 ± j22.4 that are determined by the code:

```
>> GCL =tf([330.48],[0.0126 1.89 72 1330.48])
Transfer function:
                330.5
-----------------------------------
0.0126 s^3 + 1.89 s^2 + 72 s + 1330
>> damp(GCL)
 Eigenvalue                 Damping    Freq. (rad/s)
 -2.24e+001 + 2.24e+001i    7.07e-001  3.17e+001
 -2.24e+001 - 2.24e+001i    7.07e-001  3.17e+001
 -1.05e+002                 1.00e+000  1.05e+002
```

Taking into account that for this system T_s = 0.001 sec, by applying the **Bilinear Tustin Transform** the optimal closed-loop transfer function of the system is determined in the discrete-time domain:

```
>> GdCL = c2d(GCL,0.001,'tustin')
Transfer function:
3.046e-006 z^3 + 9.137e-006 z^2 + 9.137e-006 z + 3.046e-006
-----------------------------------------------------------
              z^3 - 2.855 z^2 + 2.716 z - 0.8606
Sampling time: 0.001
>> damp(GdCL)
 Eigenvalue                 Magnitude  Equiv. Damping  Equiv. Freq.
 9.78e-001 + 2.19e-002i     9.78e-001  7.07e-001       3.17e+001
 9.78e-001 - 2.19e-002i     9.78e-001  7.07e-001       3.17e+001
 9.00e-001                  9.00e-001  1.00e+000       1.05e+002
```

It is apparent that there is a complete match between the corresponding pole location on the s-plane and on the z-plane. Both, the optimal plant analogue prototype and its optimal digital equivalent are having exactly the same relative damping of ζ = 0.707. Due to this, the controller stages are designed in the continuous-time domain and further converted into their discrete-time equivalents.

Stage 4: The two controller zeros can be placed at –22 ± j22. Then, the transfer function of the series controller stage is as follows:

$$G_S(s) = \frac{(s+22+j22)(s+22-j22)}{968(s+1000)^2} = \frac{s^2+44s+968}{968(s+1000)^2} \quad (9)$$

Usually, for the physical realization of the series controller stage two remote poles, can be added.

Stage 5: The series connection of the series robust controller $G_S(s)$ and the continuous linear prototype section of the plant as a stand alone system $G_P(s)$ results in the product of their transfer functions:

$$G_{OL}(s) = G_S(s)G_P(s) = \frac{22.314K(s^2+44s+968)}{0.0126s^3+1.98s^2+72s+1000} \quad (10)$$

Stage 6: Further, $G_{OL}(s)$ is involved in a unity feedback and the closed-loop transfer function is determined as:

$$G_{CL}(s) = \frac{22.314K(s^2+44s+968)}{\left[\begin{array}{l}0.0126s^3+1.98s^2+72s+1000+\\+22.314K(s^2+44s+968)\end{array}\right]} \quad (11)$$

Stage 7: As seen in the equation (11) the poles and the zeros of G_{CL}(s) are in close vicinity. In order to avoid the closed-loop zero-pole cancelation, a forward controller G_F(s), as presented in equation (12), is added in series to the closed-loop system. It cancels the zeros of the closed-loop transfer function G_{CL}(s).

$$G_F(s) = \frac{968}{s^2+44s+968} \quad (12)$$

Stage 8: Finally, the transfer function of the total compensated robust liner section of the system becomes:

$$G_T(s) = G_F(s)G_{CL}(s) = \frac{21.6K}{\left[\begin{array}{l}0.0000126s^3+0.00198s^2+0.072s+\\+1+0.022314K(s^2+44s+968)\end{array}\right]} \quad (13)$$

5.3. Design of the Robust Controller Stages in the Discrete-time Domain

The series and the forward robust controller stages are realized by implementing digital filters based on microcontrollers [25], [26]. Taking into account equation (9), the series robust control stage can be presented in the discrete-time domain by the following code:

```
>> Gs=tf([1 44 968],[968 1936000 968000000])
   Transfer function:
          s^2 + 44 s + 968
   -------------------------------
   968 s^2 + 1.936e006 s + 9.68e008
>> Gds=c2d(Gs,0.001,'tustin')
   Transfer function:
   0.0004693 z^2 - 0.0009181 z + 0.0004491
   ---------------------------------------
    z^2 - 0.6667 z + 0.1111
   Sampling time: 0.001
```

From the code, the transfer function of the series digital robust stage is presented in the discrete-time domain as follows:

$$G_{dS}(z)=\frac{\left[\begin{array}{l}0.0004693\ z^2-0.0009181\ z+\\+0.0004491\end{array}\right]}{z^2-0.6667\ z+0.1111}=\frac{U(z)}{X(z)} \quad (14)$$

The output of the series controller in the discrete-time domain is determined from equation (14) as:

$$\begin{aligned}U(z)=&\ 0.0004693\ X(z)\ -\ 0.0009181\ z^{-1}X(z)\ +\\&+0.0004491z^{-2}X(z)+\\&+\ 0.6667\ z^{-1}U(z)\ -\ 0.1111z^{-2}U(z)\end{aligned} \quad (15)$$

To enable the implementation of a microcontroller in the mini-loop of the system, the transfer function of the series digital robust control stage $D_{dS}(z)$, based on equation (15), is represented by the following **difference equation** [19], [25], [26]:

$$\begin{aligned}u(kT)=&\ 0.0004693\,x(kT)-0.0009181\,x\left[(k-1)T\right]+\\&+0.0004491\,x\left[(k-2)T\right]+\\&+0.6667u\left[(k-1)T\right]-0.1111u\left[(k-2)T\right]\end{aligned} \quad (16)$$

Further, considering equation (12), the transfer function of the forward robust stage can be modified by adding a zero to improve the speed of system response:

$$G_F(s)=\frac{96.8s+968}{s^2+44s+968} \quad (17)$$

Then, the forward robust control stage can be presented in the discrete-time domain by the following code:

```
>> Gf=tf([96.8 968],[1 44 968])
   Transfer function:
        96.8 s + 968
   ----------------
   s^2 + 44 s + 968
>> Gdf=c2d(Gf,0.001,'tustin')
   Transfer function:
        0.04758 z^2 + 0.0004735 z - 0.04711
   ----------------------------------
    z^2 - 1.956 z + 0.957
   Sampling time: 0.001
```

From the outcome of the applied code, the transfer function of the forward robust control stage presented in the discrete-time domain is presented as follows:

$$G_{dF}(z)=\frac{0.04758\ z^2+0.0004735z-0.04711}{z^2-1.956\ z+0.957}=\frac{V(z)}{E(z)} \quad (18)$$

The output of the forward controller in the discrete-time domain is determined from equation (18) as:

$$\begin{aligned}V(z)=&\ 0.04758\ E(z)+0.0004735\,E(z)z^{-1}-\\&-0.04711E(z)z^{-2}+\\&+1.956\ V(z)z^{-1}-0.957V(z)z^{-2}\end{aligned} \quad (19)$$

Based on equation (19), to facilitate the implementation of a forward microcontroller, the transfer function of the forward digital robust control stage $D_F(z)$ is expressed by the following **difference equation** [19], [25], [26]:

$$\begin{aligned}v(kT)=&\ 0.04758\,e(kT)+0.0004735\,e\left[(k-1)T\right]-\\&-0.04711\,e\left[(k-2)T\right]\\&+1.956\,v\left[(k-1)T\right]-0.957\,v\left[(k-2)T\right]\end{aligned} \quad (20)$$

The two-stage digital robust controller is presented as a two-stage robust microcontroller. A multiple-input multiple-output microcontroller [26], [27] can be implemented to perform this operation. One of its sections is design as a forward microcontroller, while a second section, as a series microcontroller. The system is presented in Figure 8.

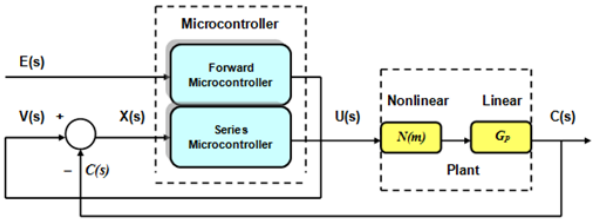

Figure 8. A Multiple-Input Multiple-Output Microcontroller Integrated into the Robust Control System

6. Advanced D-Partitioning Analysis of the Robust Linear Section of the System

Based on the characteristic equation of the total robust compensated system $G_T(s)$, the variable parameter K is determined as:

$$K(s)=-\frac{0.0126s^3+1.98s^2+72s+1000}{22.314s^2+981.818s+21599.95} \quad (21)$$

The D-Partitioning curve related to the linear section prototype of the system after the robust compensation is plotted in the discrete-time domain, as shown in Figure 9 with the aid of the following code:

```
>> K=tf([-0.0126 -1.98 -72 -1000],[22.314 981.818 21599.95])
   Transfer function:
   -0.0126 s^3 - 1.98 s^2 - 72 s - 1000
   ------------------------------------
   22.31 s^2 + 981.8 s + 2.16e004
>> Kd = c2d(K,0.001,'tustin')
   Transfer function:
   -1.193 z^3 + 3.399 z^2 - 3.226 z + 1.02
   ---------------------------------------
   z^3 - 0.956 z^2 - 0.9991 z + 0.957
   Sampling time: 0.001
>> dpartition(Kd)
```

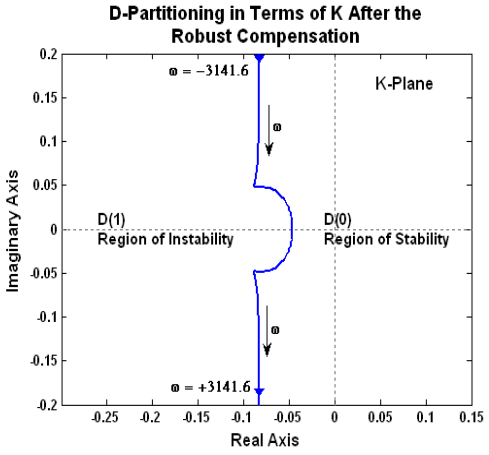

Figure 9: D-Partitioning after the Robust Compensation (Case of DC Motor Control System)

The D-Partitioning determines two regions of the *K*-plane: D(0) and D(1). As seen from Figure 9, D(0) is the region of stability, being on the left-hand side of the curve for a frequency variation within the range –3141.6 rad/sec ≤ ω ≤ +3141.6 rad/sec. Now the system is stable for any positive values of the gain, $K > 0$. If this result is compared with the one before the application of the robust compensation, it is obvious that the robust controller also improves considerably the system stability.

7. Describing Function Analysis of the Total Robust Control System

The total compensated system will be examined for robustness by the Describing Function analysis in the discrete-time domain for two gain values $K = 0.5$ and $K = 10$, submitting the gain values in equation (13). The system performance can be assessed from Figure 10 after applying the following code:

```
>> GT05=tf([0 10.8],[0.0000126 0.013 0.56 10.65])
Transfer function:
          10.8
-----------------------------------------
1.26e-005 s^3 + 0.013 s^2 + 0.56 s + 10.65
>> GdT05 = c2d(GT05,0.001,'tustin')
Transfer function:
7.016e-005 z^3 + 0.0002105 z^2 + 0.0002105 z + 7.016e-005
-------------------------------------------------------
      z^3 - 2.295 z^2 + 1.62 z - 0.3242
Sampling time: 0.001
>> GT10=tf([0 216],[0.0000126 0.222 9.75 212.96])
Transfer function:
          216
-----------------------------------------
1.26e-005 s^3 + 0.222 s^2 + 9.75 s + 213
>> GdT10 = c2d(GT10,0.001,'tustin')
Transfer function:
0.0002142 z^3 + 0.0006425 z^2 + 0.0006425 z + 0.0002142
-------------------------------------------------------
      z^3 - 1.16 z^2 - 0.5994 z + 0.7614
Sampling time: 0.001
>> nyquist(GdT05,GdT10)
```

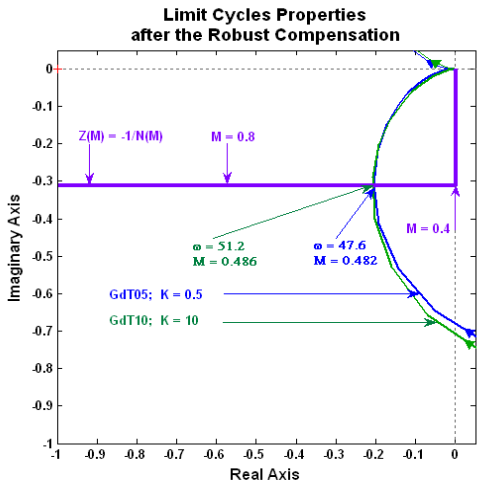

Figure 10: Interaction with the Nonlinearity after the Robust Compensation (Case of Variable Gains: K = 0.5 and K = 10)

Considering Figure 10, the stable limit cycles properties, corresponding to the intercept points between *Z(M)* and the compensated G_{dT05}, G_{dT10}, are presented in Table 3.

Table 3

Properties of the Stable Limit Cycles at Different Gains *K*

Linear Section Gain	*K*	0.5	10
Limit Cycles Properties	*M*	0.482	0.486
	ω, rad/sec	47.6	51.2

By comparing Figure 10 with Figure 6 and the results, presented in Table 3 with those of Table 2, it is seen that after the application of the robust controller the properties of the stable limit cycles differ insignificantly. The total control system becomes robust in terms of variations of the system gain *K* within specific limits.

Further research proves that systems become robust also in case of variations of any of their time-constants or their nonlinear parameters [14], [23], [25], [27].

8. Load Characteristics of the DC Motor Incorporated into the Control System

Variable load torque is achieved by mechanical coupling of the dc motor and a dc generator. A variable load resistor, in series with the generator armature, facilitates the generator to apply a variable torque to the dc motor.

Comparison of the load steady-state characteristics of the dc motor $n = f(T)$, before and after application of the feedback control, is shown in Figure 11. They have been obtained at different armature voltages V_{bc} and constant field current.

If the dc motor is not incorporated into the feedback control system, its characteristics are considerably inclined. The load steady-state characteristics of the dc motor for the case of the closed-loop system show that the motor's speed remains almost constant.

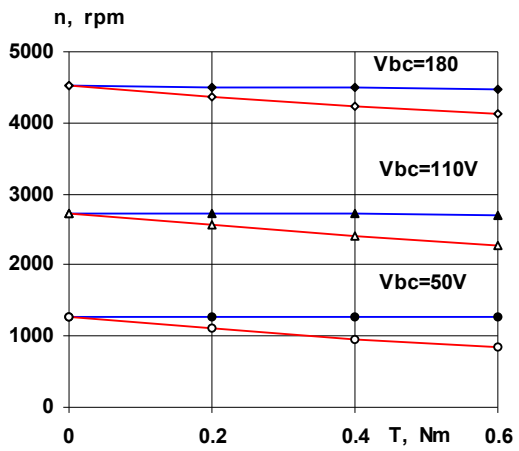

Figure 11: Load Characteristics of the DC Motor with and without the Application of the Feedback

As seen from Figure 11, for example at a load torque T_L = 0.6Nm and V_{bc} = 180V, the relative drop in the motor's speed for the case of the open-loop system is 7.78%, while for the closed-loop system it is only 1.11%. At T_L = 0.6Nm and V_{bc} = 50V the relative drop in speed is 22.8% without a feedback and 0.23% with a feedback.

9. Conclusion

Contribution of this research is the achieved further development of the Advanced D-Partitioning method in its application for the analysis and design of a digital robust control for nonlinear control systems with a low degree of nonlinearity. The results of the research demonstrate that the Advanced D-Partitioning analysis can be applied independently to the continuous linear prototype section of the system if the sampling period is at least 5 to 10 times smaller than the plant's minimum time constant. Then there will be a close match between the discrete and the continuous-time system performance. The outcome obtained from the Advanced D-Partitioning analysis, by considering only the stability of the linear prototype part of the system is an important precondition for further discussion on the interaction between the linear and nonlinear sections.

The total system performance is assessed in terms of the interaction between its linear and the nonlinear sections with the aid of the Goldfarb stability criterion, based on the Describing Function analysis. The natural and desirable operation of a control system containing a nonlinearity of the type ON-OFF element with hysteresis is yielding a stable sustained oscillation, or a stable limit cycle, with a specific amplitude and frequency. It is employed as a feedback control signal for maintaining the constant system output. It is seen that after the implementation of the robust controller, the properties of the resulting limit cycles differ only insignificantly, maintaining the robustness of the total control system.

A major advantage of the Describing Function analysis is the graphical display and the simplicity of its application for systems with complex dynamics in their linear parts. The Describing Function analysis can be considered as a linear approximation of a static nonlinearity limited to the first harmonic. Although considered as an approximate tool, by applying it, useful results with practical accuracy are achieved.

Comparison between adaptive and robust control reveals that the while adaptive control cannot be applied in case of unstructured and unpredictable uncertainties, a robust controller can be implemented for unpredictable parameter variations. Anticipating random parameter uncertainties in the system under discussion, an optimal robust controller is preferred. It is designed by applying a number of unique successive steps and achieving forward-series compensation with two degrees of freedom. The controller enforces the desired system performance.

Analysis in the discrete-time domain before and after the application of the robust controller proves that the system becomes quite insensitive to its parameter variations. To achieve digital robust control, the transfer functions of the two controller stages are presented by their difference equations. Microcontrollers are incorporated into the control system as forward and series robust control stages and can be programmed to solve their related difference equations. The two-stage robust microcontroller is achieved by employing a multiple-input multiple-output microcontroller. Since, for the discussed case, the system's sampling period is 0.001sec, the sampling frequency of operation is 1 kHz. That can be managed successfully by some of the latest microcontrollers operating at frequency up to 200 MHz.

Further experiments prove that if the dc motor is incorporated into the feedback control system its speed remains almost constant, in this way achieving a very accurate speed control.

The suggested technique for the system's analysis by implementing the innovative Advanced D-Partitioning method and the design of robust control by applying a number of distinctive successive steps can be useful for further development of control theory in this area and effective for practical implementation.

10. References

[1] Yanev K.M., Anderson G.O., Masupe S., Strategy for Analysis and Design of a Digital Robust Controller for Nonlinear Control Systems, 4th IASTED International Conference, ISBN 978-0-88986-929-5, p. 213-220. 2012

[2] Neimark Y., D-partition and Robust Stability, Computational Mathematics and Modeling, Vol. 9(Issue 2), pp. 160-166, 2006.

[3] Yanev K.M., Application of the Method of the D-Partitioning for Stability of Control Systems with Variable Parameters, Botswana Journal of Technology, Vol. 15(Issue 1): 26-33, 2005.

[4] Bilinear Transform, Retrieved January 17, 2016 from http://en.wikipedia.org/wiki/Bilinear_transform.

[5] Euler Method, Retrieved January 17, 2016 from http://en.wikipedia.org/wiki/Euler_method.

[6] Continuous to Discrete Conversion Methods, Retrieved January 17, 2016 from http://www.mathworks.com/help/control/ug/continuous-discrete-conversion-methods.html#bs78nig-1.

[7] Yanev K.M., Advanced Interactive Tools for Analysis and Design of Nonlinear Robust Control Systems, International Review of Automatic Control (IREACO), ISSN: 1974-6059, Vol. 6, N. 6, pp. 720-727, 2013.

[8] Yanev K.M, Anderson G., Multivariable System's Parameters Interaction and Robust Control Design, International Review of Automatic Control (IREACO), Napoli, Italy, Vol. 4, N.2, ISSN: 1974-6059, pp. 180-190, 2011.

[9] Yanev K.M., Analysis of Systems with Variable Parameters and Robust Control Design, Proceedings of the 6th IASTED International Conference on Modeling, Simulation and Optimization, pp. 75-83, 2006.

[10] Neimark Y., Robust stability and D-partition, Automation and Remote Control 53(7), pp. 957–965, 1992.

[11] Gryazina E. Polyak B., Stability Regions in the Parameter Space: D-Decomposition Revisited, Moscow, Russia, Automatica, 13–26, 2006.

[12] Yanev K. M., Application of the Method of D-Partitioning for Stability of Control Systems with Variable Parameters, BJT, Vol.16, Number 1, pp.51-58, 2007.

[13] Yanev, K.M., Anderson G.O., Masupe S., D-Partitioning Analysis and Design of a Robust Photovoltaic Light Tracker System, BIE 12th Annual Conference, 6001, ISBN: 97899912-0-731-5, 2011.

[14] Yanev K.M., Advanced Interactive Tools for Analysis and Design of Nonlinear Robust Control Systems, International Review of Automatic Control, ISSN: 1974-6059, Vol. 6, N. 6, pp. 720-727, 2013.

[15] Yanev K. M., Anderson G. O., Masupe S., Strategy for Analysis and Design of Digital Robust Control Systems, ICGST-ACSE Journal, Volume 12, Issue 1, pp. 37-44, 2012.

[16] Tustin with Frequency Prewarping. MathWorks R2014b Documentation. Retrieved October 17, 2014, http://radio.feld.cvut.cz/matlab/toolbox/control/manipmod/ltiops20.html

[17] Phillips C., Digital Control System, Prentice- Hall International Inc., pp.125-403, 2005.

[18] Dorf R.C., Modern Control Systems, New York, USA, Addison-Wesley, pp.578-583, 2006.

[19] Bhanot S., Process Control Principles, Oxford University Press, pp. 170-187, 2010.

[20] Landau I.D., Adaptive Control Algorithms and Applications, Springer, ISBN: 978-0-85729-663-4, 2011, pp.1-587, 2011.

[21] Ioannou, P.A., Robust Adaptive Control, PTR Prentice-Hall, Upper Saddle River NJ, pp.1-825, 2007.

[22] Adaptive control. In Wikipedia, Retrieved September 7, 2014, from http://en.wikipedia.org/wiki/Adaptive_control

[23] Yanev K.M., Analysis and Design of a Servo Robust Control System, International Review of Automatic Control, ISSN: 1974-6059, Vol. 7, N. 2, pp. 217-224, 2014.

[24] Shinners S., Modern Control System Theory and Application, Addison Wesley Publishing Company, London, pp. 43-46, 2008.

[25] Architecture and programming of 8051 MCU's, Retrieved January 14, 2015, from http://www.mikroe.com/chapters/view/64/chapter-1-introduction-to-microcontrollers/

[26] Bates M., Interfacing PIC Microcontrollers, Elsevier, London, UK, pp. 55-168, 2006.

[27] PIC microcontroller, Retrieved January 17, 2016 from https://en.wikipedia.org/wiki/PIC_microcontroller.

Biographies

[1]Prof. Kamen Yanev started his academic career in 1974, following a number of academic promotions and being involved in considerable research, service and teaching at different Commonwealth Universities around the world. He also worked in a number of universities in Europe and in Africa, in countries like Nigeria, Zimbabwe and Botswana. The PhD of Prof. Yanev is in the area of Systems with Variable Parameters and Robust Control Design. Currently he works as Associate Professor in Control and Instrumentation Engineering at the Department of Electrical Engineering at University of Botswana.

His major research is in the field of Control Engineering as well as in the subjects of Electronics and Instrumentation. He has more than 110 publications in international journals and conference proceedings in the area of Control Engineering, Electronics, Instrumentation and Power Engineering. Most of his latest publications and current research interests are in the field of Electronics, Analysis of Control Systems with Variable Parameters and Robust Control Design.

Prof. Yanev is a member of the Institution of Electrical and Electronic Engineering (IEEE), a member of the Academic Community of International Congress for Global Science and Technology (ICGST), interacting with Saint-Cyr French Military Academy, a member of the Instrumentation, Systems and Automation Society (ISA), a member of the Editorial Board of the International Journal of Energy Systems, Computers and Control (IJESCC), at International Science Press, a member of the Editorial Board of the Journal of Multidisciplinary Engineering Science and Technology (JMEST), a reviewer for ACTA Press (a Scientific and Technical Publishing Company), and a member of the Botswana Institute of Engineers (BIE).